

Macroscopic Properties of Open-Cell Foams Based on Micromechanical Modelling

M. Janus-Michalska and R. B. Pecherski

This paper presents a micromechanical analysis for the assessment of macroscopic behaviour of three-dimensional open-cell solid foams. The analysis is based on material properties of a solid phase and topological arrangement of cell structure. A foam structure consists of idealized tetrahedral unit cells, which are built of four identical half-struts forming a diamond-like structure and identified as Plateau borders. Such a unit cell represents the essential microstructural features of foam. An analytical formulation of force-displacement relations for struts can be found by considering the affinity of node displacements in tensile, bending, and shear deformation. The elements of the stiffness matrix for a single cell are expressed as functions of the compliance coefficients for stretching and bending of struts. The effective elastic constants for metallic foam considered as isotropic material are determined as functions of foam relative density and compared with available results. In this paper we define an energy-based limit condition of linear elasticity for open-cell foams and calculate the critical energy density pertinent to a particular orthogonal energy state accounting for elementary interactions in a microstructure. The study based on the assumption of linear elasticity leads to simple analytical formulas. Nevertheless, it should be stressed that the proposed theoretical basis of micromechanical modelling could be also applied for the analysis of nonlinear elastic behaviour, plasticity, and failure of foams. Such problems require, however, a more complex numerical approach.

1 Introduction

The term “solid foams” is commonly used for describing three-dimensional cellular materials with a highly dispersive solid phase arranged into cells - polyhedra, which fill the three-dimensional space. The cells can be either open or closed. Such a kind of structure can be found in many natural materials, for example cork, wood, and cancellous bone. High technology foams are manufactured from polymers, ceramics, and metals and can be used in reinforced lightweight structures, packaging, and crash-protection systems. Because of their structure natural and synthetic cellular solids show unique physical properties, which provide their optimal functionality. The development of mechanics of cellular solids is documented in Gibson and Ashby (1998). In order to develop new materials it is necessary to understand better the mechanism of foam deformation. We assume that essential macroscopic features of mechanical behaviour of open-cell foams can be inferred from the deformation response of a representative microstructural element. The properties of cellular solids depend on material from which they are made, internal geometrical structure and relative density ϕ . By relative density ϕ we understand a quotient of density of cellular material and density of the solid from which the cells are made; i.e. the cell edges, in case of open-cell foams, or cell walls for closed-cell foams. A value of foam relative density is usually less than 0.3; and about 0.001 for ultra-low-density special foams. Above the value of about 0.3 the pore space shrinks and transformation into a porous material occurs (Gibson and Ashby, 1998). To model a random microstructure and evaluate its mechanical properties in macroscopic scale a simple periodic structure can be assumed in the first step. The aim of the paper is to develop a constitutive description of the linear elastic behaviour of open-cell foams on the basis of microstructural modelling of a foam skeleton. The study is related to effective models construction (Phillips, 2001). We also propose an energy-based limit criterion and the critical values of energy density that are calculated from the discussed microstructural model. Early works on elastic foam mechanics belong to Gent and Thomas (1959, 1963). The authors assumed that struts in a foam skeleton transmitted axial load only. A number of later analytical studies have incorporated bending deformation of struts (Choi and Lakes, 1995; Gibson and Ashby, 1982; Ko, 1965; Menges and Knipschild, 1975; Warren and Kraynik, 1987, 1997, 1998), which is understood to be a dominant deformation mechanism for small deformations of open-cell foam. In the analysis in Warren and Kraynik (1997) torsion of a strut was also included.

1.1 Topological Arrangement of Foam Cell Structure and Foam Morphology

The topology and morphology of foam microstructure reflect a method of its preparation, which usually involves a continuous liquid phase that eventually solidifies and therefore surface tension and related interfacial effects often control the foam structure. There are two well known elementary features of the liquid foam structure that are required to minimize surface energy. According to Bikerman (1973), three films always meet at equal angles of 120° to form a film junction called Plateau border (cf. Gibson and Ashby (1998), where the work of J.A.F.

Plateau (1873) is cited). Four Plateau borders always join at the tetrahedral angle of 109.47° . For open cell foams Plateau borders are identified as foam skeleton struts (Warren and Kraynik, 1998). Also in a closed-cellular structure, if the films are very thin compared to the struts, the similar response to open-cell foam is expected.

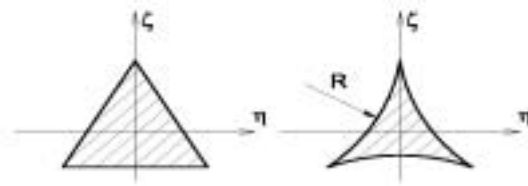


Fig. 1. The considered strut cross-sections: a. equilateral triangle; b. Plateau border

The struts originate from liquid in Plateau borders, which form along the edges of polyhedral cells. Surface tension, viscous flow and other physico-chemical mechanisms control the evolving strut geometry during foam formation when gas bubbles grow and deform in a highly viscous liquid, which eventually solidifies. The films are required to be very thin in comparison to the transverse dimension of struts. For low-density foams with long struts the cross section can be assumed as an equilateral triangle or Plateau border as shown in Fig. 1. The considered struts with cross-sections of shapes of an equilateral triangle or Plateau border have threefold axis of geometric symmetry. This affects the material symmetry of a unit cell. No cell in three-dimensional foam is a simple polyhedron with planar faces and straight edges. Tetrahedra do not fill out the space so our geometric assumptions are not precisely compatible with any three-dimensional network of struts, cf. Gibson and Ashby (1998); however, even though the results cannot be exact they provide useful insight into foam mechanics.

1.2 Micromechanical Models

Two micromechanical models are known in literature. The first one, based on a tetrahedral element, was adopted by Warren and Kraynik (1998); the representative tetrahedral element consists of four identical half struts that meet at equal tetrahedral angles. This choice of a microstructural element is consistent with the topological feature of foam given previously. The relative orientation of adjacent tetrahedral elements that possess a common strut is assumed to be random. The boundaries of unit cell consist of four planes that are perpendicular to each strut at its midpoint and form a regular tetrahedron. This model enables us to obtain only averaged elastic constants over all possible orientations and to estimate the elastic properties of the foam. According to Gibson and Ashby (1998), Lord Kelvin (W. Thompson) showed in 1887 that space could be partitioned into identical tetrakaidecahedral cells of equal volume and minimal surface area. A tetrakaidecahedron has six quadrilateral and eight non-planar hexagonal surfaces all with curved edges. This model is referred to as Kelvin foam and was adopted by Zhu et al. (1997) as well as Warren and Kraynik (1997). Predicted elastic properties of the Kelvin foam model are not isotropic, for the Young modulus E varies of about 10% with change of direction. In most existing foams, however, there are no distinguished directions regarding their microstructure and one should expect isotropy as elastic properties are concerned. The Kelvin foam model exhibits also an unusual behaviour that has not been confirmed in real materials; for example, a value of Poisson's ratio corresponds to incompressibility $\nu=0.5$, which is not a true value. Gibson and Ashby (1998) found large scattering of experimental data for Poisson's ratio. Experiments show its dependence on the skeleton material and foam morphology but no dependence on density. The value $\nu=0.5$ has not been obtained as a result of experiment.

In this work we assume that the analysis of the deformation of a representative tetrahedral element without any assumption concerning cell orientation captures essential features of the mechanical response. We also assume that the deformation of cells under uniform strain states is affine. It results in affinity of film midpoint or strut midpoint displacements. According to Warren and Kraynik (1998) we note that strict affine deformation is a consequence of a perfectly ordered structure and cannot be expected in foams that are polydisperse or are disordered in another way. The affinity assumption is justified by the results of observation of foam under a microscope (Menges and Knipschild, 1975); foam is regarded as a special kind of an ordered structure, which approximately fills out the space.

2 Micromechanical Analysis

2.1 Unit Cell

We model three-dimensional foam with the smallest repetitive element, which defines a spatially periodic structure. Microstructural mechanical features of an open-cell foam are represented by a tetrahedral unit cell with a skeleton of four half struts of length $L/2$, which meet in the point O with the tetrahedral angle of 109.47° . As it

is shown in Fig. 2, the struts are perpendicular to the cell faces. We choose such a position of the unit cell, with respect to the unit vectors $\vec{e}_\alpha, \alpha = x, y, z$ of the assumed coordinate system, which is especially suitable for the analysis.

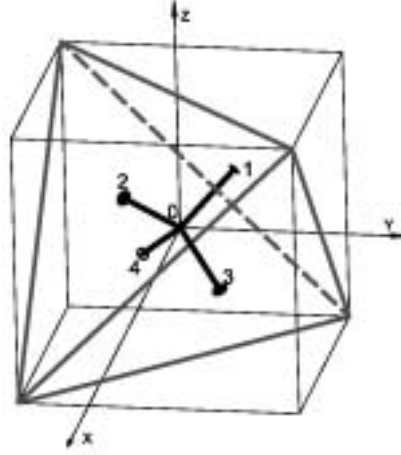


Fig. 2. An idealized tetrahedral unit cell built of four identical half-struts forming a diamond-like structure

The strut midpoints are described then in a simple way by the following position vectors $\vec{b}_i^0, i = 1, \dots, 4$

$$\begin{aligned} \vec{b}_1^0 &= \left(-L \frac{\sqrt{3}}{6}, L \frac{\sqrt{3}}{6}, L \frac{\sqrt{3}}{6} \right) & \vec{b}_2^0 &= \left(L \frac{\sqrt{3}}{6}, -L \frac{\sqrt{3}}{6}, L \frac{\sqrt{3}}{6} \right) \\ \vec{b}_3^0 &= \left(L \frac{\sqrt{3}}{6}, L \frac{\sqrt{3}}{6}, -L \frac{\sqrt{3}}{6} \right) & \vec{b}_4^0 &= \left(-L \frac{\sqrt{3}}{6}, -L \frac{\sqrt{3}}{6}, -L \frac{\sqrt{3}}{6} \right) \end{aligned} \quad (1)$$

A solid skeleton modeled with struts structure that is oriented in accordance with Fig. 2 corresponds to a diamond-like structure and has, consequently, cubic symmetry. It can be proved by the fact that a composition of three transformations: right angle rotation with respect to axis α (where $\alpha = x, y, z$) with mirror reflection with respect to the plane that is perpendicular to the given axis α , gives the same structure. A transformation law for the fourth order elasticity tensor gives relations for stiffness matrix components typical for cubic symmetry (Nalepka, ...). It is worth reminding that such a regular cell is an idealization; however, it leads to a simple analytical description. Irregular cells are often observed; members of different length and/or subtending various relative angles form them. Additionally, different mechanical properties can be assumed for each of the members in a cell solid skeleton. The effects of geometry of such irregular cells on anisotropy of foams are analyzed in Wang and Cuitiño (2000). The estimation of elastic properties of model random three-dimensional open-cell solids for different cellular structures with use of FEM analysis is presented in Roberts and Garboczi (2002).

2.2 Kinematics of a Unit Cell

The following analysis is based on the discussed above model of a representative unit cell and the assumption of infinitesimal displacements, uniform strains, and midpoint displacement affinity. Let us consider uniaxial extension ε_α in the direction $\alpha = x, y, z$ of a unit cell (an example is shown in Fig.3a). For such a deformation the strut midpoint relative displacements are given by the following formula:

$$\bar{\Delta}_i(\varepsilon_\alpha) = \varepsilon_\alpha (\vec{b}_i^0 \cdot \vec{e}_\alpha) \vec{e}_\alpha \quad i = 1, \dots, 4 \quad (3)$$

For pure shear $\gamma_{\alpha\beta}$ in the $\alpha\beta$ plane ($\alpha \neq \beta$), Fig 3b, the relative displacements are given as follows:

$$\bar{\Delta}_i(\gamma_{\alpha\beta}/2) = (\gamma_{\alpha\beta}/2) \left((\vec{b}_i^0 \cdot \vec{e}_\alpha) \vec{e}_\beta - (\vec{b}_i^0 \cdot \vec{e}_\beta) \vec{e}_\alpha \right) \quad i = 1, \dots, 4 \quad (4)$$

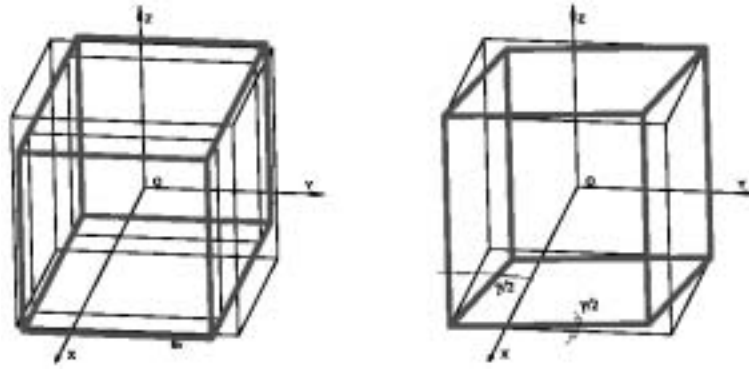


Fig.3. Deformation of a unit cell: a) uniaxial extension in x direction; b) pure shear in x-y plane

Displacements obtained in such a way can be represented by the components that are normal and tangent to the individual strut direction (in the plane of tetrahedral wall).

$$\bar{\Delta}_i = \bar{\Delta}_m + \bar{\Delta}_{\tau} \quad (5)$$

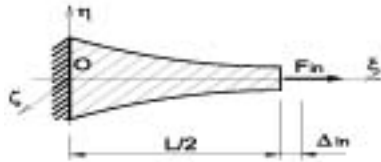
where the displacement components can be obtained by use of the following formulas:

$$\bar{\Delta}_m = (\bar{\Delta}_i \cdot \bar{e}_i) \bar{e}_i \quad \bar{\Delta}_{\tau} = (\bar{\Delta}_i \times \bar{e}_i) \times \bar{e}_i.$$

2.3 Force-Displacement Relations of a Foam Skeleton

The model of Timoshenko beam is adopted as the most appropriate for short struts of the foam skeleton; while for low-density foams with long, slender struts the Bernoulli-Euler beam theory was satisfactory. At this level we can take into account a non-uniform morphology. This is the case where the transverse strut dimension varies gradually along the centerline axis with the maximum value at the joint and the minimum in the midpoint.

As a consequence of the assumed displacement affinity we find that individual strut deforms antisymmetrically with respect to its midpoint so the resultant bending moment at the midpoint disappears. The elastic behaviour of a cantilever beam under axial and transverse load is known from classical solutions; for axial load the differential equation with boundary condition is to be solved:



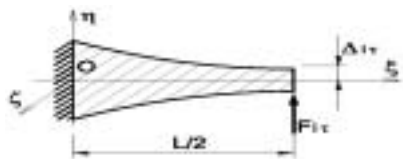
$$\frac{d}{d\xi} (\Delta_m(\xi)) = \frac{N(\xi)}{E_s A(\xi)}, \quad \Delta_m(0) = 0 \quad (6)$$

Fig. 4. A representative non-uniform strut subjected to axial load.

where $N(\xi) = F_{in}$ is the axial force, $\Delta_m = \Delta_m(L/2)$ denotes the midpoint axial displacement and E_s corresponds to the Young modulus for a skeleton material. The solution shows that force-displacement relation is linear with coefficient s_n determined as the axial elastic beam stiffness while the elastic compliance is defined as $c_n = s_n^{-1}$. For uniform cross-section we have:

$$c_n = \frac{L}{2E_s A} \quad (7)$$

For non-uniform cross-section elastic beam compliance becomes a function of foam morphology. A solution for transverse load shows that for a cantilever beam a displacement-force relation is also linear with the coefficient c_τ defined as bending elastic strut compliance. For transverse load the differential equation with boundary conditions for a Bernoulli-Euler beam, where deflections depend only on bending moments, reads:



$$\frac{d^2}{d\xi^2} ({}^M \Delta_{\tau}(\xi)) = \frac{M(\xi)}{E_s J(\xi)}, \quad {}^M \Delta_{\tau}(0) = 0, \quad \frac{d}{d\xi} ({}^M \Delta_{\tau}(0)) = 0 \quad (8)$$

Fig. 5. A representative non-uniform strut subjected to transverse load.

$M(\xi) = F_{it} \left(\frac{L}{2} - \xi \right)$ is a function of the bending moment and ${}^M \Delta_{it} = {}^M \Delta_{it} \left(\frac{L}{2} \right)$ denotes the midpoint transverse displacement. For a Timoshenko beam the additional displacement component related to shear stress should be included. It can be obtained as a solution of the following differential equations with boundary conditions:

$$\frac{d}{d\xi} \left({}^o \Delta_{it}(\xi) \right) = \frac{Q(\xi)}{G_S A_\tau(\xi)}, \quad {}^o \Delta_{it}(0) = 0 \quad (9)$$

Where $Q(\xi) = F_{it}$, ${}^o \Delta_{it} = {}^o \Delta_{it} \left(\frac{L}{2} \right)$ and $A_\tau(\xi) = \frac{J(\xi) b(\xi)}{S(\xi)}$ are geometric characteristics of the beam cross-section. The bending elastic compliance is a sum of two components. The first one corresponds to the Bernoulli-Euler beam response, whereas the other one is related to shear strains in a Timoshenko beam. For a uniform cross-section the solution reads:

$$c_\tau = \frac{L^3}{24 E_S J} + \frac{L}{2 G_S A_\tau} \quad (10)$$

The bending stiffness of beams is given by $s_\tau = c_\tau^{-1}$ and then force-displacement relations

$$F_{in} = \Delta_m \cdot s_n, \quad F_{it} = \Delta_{it} \cdot s_\tau, \quad i = 1, \dots, 4 \quad (11)$$

enable us to obtain normal and transverse forces in case where displacements from the deformation analysis are given. The components of internal forces obtained in such a way fulfill the equilibrium conditions:

$$\sum_{i=1}^4 \vec{F}_i = 0 \quad \sum_{i=1}^4 \vec{F}_i \times \vec{b}_i^0 = 0. \quad (12)$$

2.4 Effective Stress Tensor Definition

Cutting the representative volume element with plane $\pi : x = 0$ and considering the effective stress that has to act upon the exposed face to maintain the equilibrium with forces on the remaining volume gives the following equilibrium equation:

$$A_x (\sigma_{xx} \vec{e}_x + \sigma_{xy} \vec{e}_y + \sigma_{xz} \vec{e}_z) + \vec{F}_1 + \vec{F}_4 = 0 \quad (13a)$$

An analogical cutting with use of $\pi : y = 0$, as illustrated in Fig.7, results in the following equation:

$$A_y (\sigma_{yx} \vec{e}_x + \sigma_{yy} \vec{e}_y + \sigma_{yz} \vec{e}_z) + \vec{F}_2 + \vec{F}_4 = 0 \quad (13b)$$

Similarly, cutting with use of plane $\pi : z = 0$ gives:

$$A_z (\sigma_{zx} \vec{e}_x + \sigma_{zy} \vec{e}_y + \sigma_{zz} \vec{e}_z) + \vec{F}_3 + \vec{F}_4 = 0 \quad (13c)$$

where $A_x = A_y = A_z = A = \frac{3}{2} L^2$ for the square sections and $\vec{e}_x, \vec{e}_y, \vec{e}_z$ are the unit vectors associated with the coordinate system. The solution of the set of equations (13) gives the stress tensor components.

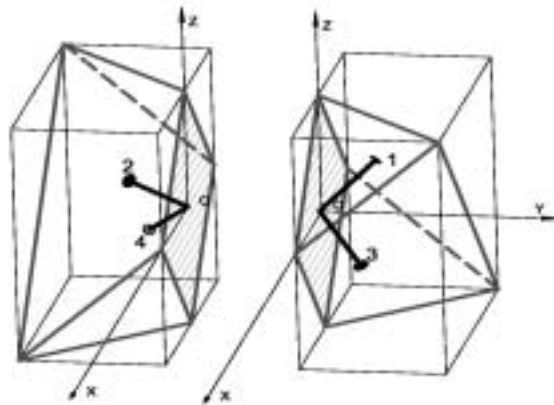


Fig. 6. The way of calculating the effective stress tensor components.

2.5 Effective Elasticity Tensor

On the basis of the previous analysis an effective constitutive matrix for the unit cell is constructed. Since the symmetry of the unit cell is cubic the following matrix represents the elasticity tensor, (axes x, y, z are related respectively with indices 1, 2, 3):

$$\underline{\mathbf{S}} = \begin{bmatrix} s_{1111} & s_{1122} & s_{1122} & 0 & 0 & 0 \\ s_{1133} & s_{1111} & s_{1122} & 0 & 0 & 0 \\ s_{1122} & s_{1122} & s_{1111} & 0 & 0 & 0 \\ 0 & 0 & 0 & 2s_{1212} & 0 & 0 \\ 0 & 0 & 0 & 0 & 2s_{1212} & 0 \\ 0 & 0 & 0 & 0 & 0 & 2s_{1212} \end{bmatrix} \quad (14)$$

For cubic symmetry we have three eigenvalues (Kelvin moduli) [17-19]:

$$\lambda_I = \lambda_1 = s_{1111} + 2s_{1122}, \quad \lambda_{II} = \lambda_2 = \lambda_3 = s_{1111} - s_{1122}, \quad \lambda_{III} = \lambda_4 = \lambda_5 = \lambda_6 = 2s_{1212}$$

Two types of specific deformation are considered: uniaxial extension in x direction $\epsilon_x \neq 0$ and pure shear $\gamma_{xy} \neq 0$. As a result, the following elasticity coefficients are obtained as functions of axial and bending stiffness of the skeleton strut:

$$s_{1111} = \frac{2(s_n + 2s_\tau)}{9\sqrt{3}L}, \quad s_{1122} = \frac{2(s_n - s_\tau)}{9\sqrt{3}L}, \quad 2s_{1212} = \frac{2s_\tau}{3\sqrt{3}L} \quad (15)$$

The calculated Kelvin moduli are as follows:

$$\lambda_I = \lambda_1 = s_{1111} + 2s_{1122} = \frac{2s_n}{3\sqrt{3}L}, \quad \lambda_{II} = \lambda_2 = \lambda_3 = s_{1111} - s_{1122} = \frac{2s_\tau}{3\sqrt{3}L}$$

$$\lambda_{III} = \lambda_4 = \lambda_5 = \lambda_6 = 2s_{1212} = \frac{2s_\tau}{3\sqrt{3}L} \quad (16)$$

Since $\lambda_{II} = \lambda_{III}$ the analysis leads to an important conclusion that the considered representative cell is elastically isotropic, which in turn leads to the following consequences:

- the elastic behaviour is described by two Kelvin moduli
- the orientation of a cell can be arbitrary
- the macroscopic Kelvin moduli for foam are identical with moduli of a representative unit cell.

The above derived elastic isotropy results from the symmetry of the struts cross-sections, Fig. 1.

2.6 Macroscopic Elastic Properties

The first eigenvalue refers to bulk modulus $\lambda_I = 3K$. It can be expressed as a function of skeleton stiffness, which depends on skeleton morphology and the material of which the skeleton is built. Bulk modulus is a linear function of foam relative density $K = \alpha_K E_s \phi$, where α_K is a linear coefficient and does not depend on the type of cross-section of a foam skeleton. For uniform cross-section the bulk modulus reads $K = \frac{2E_s}{9} \phi$, where

$\phi = \frac{2A}{\sqrt{3}L^2}$ for low-density foam $\phi \ll 1$ (usually $\phi < 0.05$). The second eigenvalue is interpreted as a shear modulus $\lambda_{II} = 2G$. For a uniform cross-section and low-density foam it assumes the following form

$$2G = \frac{2s_\tau}{3\sqrt{3}L} = \frac{\beta_G \phi^2}{1 + \delta_G \phi}, \quad (17)$$

where coefficients β_G, δ_G depend on the type of the strut cross-section and its nonuniform distribution along the axis. β_G, δ_G reach higher values for short skeleton struts in the Timoshenko model than in the considered Bernoulli-Euler model because additional terms responsible for shear modes are to be taken into account. The Young modulus and Poisson's ratio can be calculated using the two latter constants from the following general

formula:

$$E = \frac{2s_n s_\tau}{\sqrt{3}L(2s_n + s_\tau)} = \frac{\beta_E \phi^2}{1 + \delta_E \phi}, \quad (18)$$

where coefficients β_E, δ_E depend on the type of strut cross-section and its nonuniformity. For low density foams the Young modulus can be approximated with a relation $E = \beta_E \phi^2$. For open-cell foam experiments show that the Young modulus can be approximated as: $E \cong E_S \cdot C_E \cdot \phi^2$, where constant C_E is calibrated from tests, E_S is the Young modulus of solid skeleton material. On the basis of microstructural analysis we can explain why this formula is only an approximation and say how accurate it is. We can also give an explicit formula for constant C_E , which is a function of microstructure morphology. According to Gibson and Ashby (1998), $C_E \approx 1$ for low-density foams, while in the case of higher density foams $C_E < 1$, as the nodes contain a significant portion of the material that is not used in a structural sense since it carries little or no load. The Poisson's ratio $\nu = \frac{s_n - s_\tau}{(2s_n + s_\tau)}$ does not depend on the foam relative density but only on the type of a cross-section and morphology.

2.7 Comparison with Other Models

Results obtained by application of the presented model can be compared with results that refer to the tetrahedral random model given in Warren and Kraynik (1998) and the Kelvin foam model given in Zhu et al. (1997). In each case low-density foam is assumed and the Bernoulli-Euler model of strut with a uniform cross-section is adopted. A comparison of the three models is given in Table 1. Other models known in literature and their comparison with FEM calculations performed for random three-dimensional open-cell solids are thoroughly discussed in Roberts and Garboczi (2002).

	Presented model	Tetrahedral model according to Warren and Kraynik (1998)	Kelvin foam model according to Zhu et al. (1997)
C_E triangle	1.0	1.1	0.726*
C_E Plateau border	1.39	1.54	0.979*
E triangle	$E = \frac{1.0 \phi^2}{1+0.5\phi} E_S$	$E = \frac{1.056 \phi^2}{1+2.98\phi} E_S$	$E_{100} = \frac{0.726 \phi^2}{1+1.09\phi} E_S$
E Plateau border	$E = \frac{1.39 \phi^2}{1+0.695\phi} E_S$	$E = \frac{1.53 \phi^2}{1+4.325\phi} E_S$	$E_{100} = \frac{1.009 \phi^2}{1+1.514\phi} E_S$
ν triangle	$\nu = 0.5 \left(\frac{1-\phi}{1+0.5\phi} \right)$	$\nu = 0.5 \left(\frac{1-0.193\phi}{1+2.98\phi} \right)$	$\nu_{12} = 0.5 \left(\frac{1-1.514\phi}{1+1.514\phi} \right)$
ν Plateau border	$\nu = 0.5 \left(\frac{1-1.45\phi}{1+0.729\phi} \right)$	$\nu = 0.5 \left(\frac{1-0.280\phi}{1+4.321\phi} \right)$	$\nu_{12} = 0.5 \left(\frac{1-1.09\phi}{1+1.09\phi} \right)$
K	$K = \frac{2}{9} \phi E_S$	$K = \frac{1}{9} \phi E_S$	$K = \frac{1}{9} \phi E_S$

Table1. Comparison of three discussed models; * denotes the model, which reveals slight anisotropy.

2.8 Specification of Energy-Based Limit Condition of Linear Elasticity for Open-Cell Foams

The analysis of compression tests carried out on specimens made of different kinds of open-cell foams shows that a linear elasticity range transforms into a range of non-linear elastic behaviour followed by permanent strains Gibson and Ashby (1998). Modelling of a foam microstructure with the help of the linear elasticity theory enables us to predict the macroscopic limit condition of linear elasticity for open-cell foams. An energy-based approach to limit conditions for isotropic solids was firstly proposed by Maxwell (1936) and Beltrami (1885), then derived independently by Huber (1904) and further developed for solids of arbitrary anisotropy by Rychlewski (1984b, 1995). The Rychlewski limit condition is based on the concept of energy orthogonal elastic stress states, which makes it possible to decompose additively the elastic energy density stored in an anisotropic body into not more than six disjoint parts. In Nalepka and Pecherski (2002) a new idea is proposed to specify the

Rychlewski criterion by analytical calculation of the critical energy density, pertinent to a particular orthogonal energy state, with an account of elementary interactions in microstructure. As an example, evaluation of critical energy density of breaking atomic bonds with application of a quantum-mechanical model of an ideal Cu nanostructure was studied in Nalepka and Pecherski (2002).

A similar approach can be also applied in defining the limit condition for open-cell foams. The elaborated microscopic model enables us to calculate the critical energy density for proper elastic states related with the change of volume and distortion. The specification of energy-based criterion for isotropic open-cell foam takes the following form:

$$\frac{I}{2K} \frac{\sigma^2}{\Phi_{CR1}} + \frac{I}{4G} \frac{\underline{S} \cdot \underline{S}}{\Phi_{CR2}} \leq 1 \quad (19)$$

where $\sigma = \frac{1}{3} tr \underline{\sigma}$ is a hydrostatic part of the stress tensor $\underline{\sigma}$ and $\underline{S} = \underline{\sigma} - \sigma \underline{I}$ is its deviator, while Φ_{CR1} stands for critical energy density in an elastic hydrostatic state of stress and Φ_{CR2} corresponds to critical energy density in a deviatoric state of stress. This criterion is formulated on a macroscopic level for the stress tensor $\underline{\sigma}$ that is defined for foam as a continuum medium. Our aim is to calculate the energy limits Φ_{CR1} and Φ_{CR2} from a microstructural model. On the microscopic level the stress in the skeleton material is denoted with the upper index "s". We adopt the well-known Huber-Mises hypothesis of elastic energy of distortion:

$${}^s \Phi_f = \frac{1+\nu_s}{6E_s} \left[({}^s \sigma_\xi - {}^s \sigma_\eta)^2 + ({}^s \sigma_\eta - {}^s \sigma_\zeta)^2 + ({}^s \sigma_\xi - {}^s \sigma_\zeta)^2 + 6({}^s \tau_{\xi\eta}^2 + {}^s \tau_{\xi\zeta}^2 + {}^s \tau_{\eta\zeta}^2) \right] \quad (20)$$

for elastic isotropic solid skeleton material, while in an uniaxial case the critical energy density for the skeleton material with the elasticity limit R_e is given by

$${}^s \Phi_f = \frac{1+\nu_s}{3E_s} R_e^2. \quad (21)$$

Let us study the following algorithm: firstly, we assume two proper elastic states and then, considering them independently, we calculate forces in the skeleton struts for each state respectively. A stress state in foam is critical when elastic energy density of distortion (20) reaches the critical value (21) for a considered skeleton. From analysing such a critical state of stress in foam as a continuum we obtain the desired critical energy density.

The first proper state: a hydrostatic state of stress results only in normal forces in each of the skeleton struts:

$$F_m(\sigma \underline{I}) = \frac{\sqrt{3}L^2}{4} \sigma \quad (22)$$

It also gives only normal stresses in the skeleton struts:

$${}^s \sigma_\xi(\sigma \underline{I}) = \frac{\sqrt{3}L^2}{4A} \sigma \quad (23)$$

When normal stress reaches the critical value:

$${}^s \sigma_{\xi CR} = \frac{\sqrt{3}L^2}{4A_{min}} \sigma = R_e \quad (24)$$

the critical hydrostatic stress in foam can be expressed as follows:

$$\sigma_{CR1} = \sigma_{CR}(\sigma \underline{I}) = R_e \cdot \frac{4A}{\sqrt{3}L^2} \quad (25)$$

The energy limit for the first proper state, which is derived on the basis of the above microscopic analysis, can be also given by the explicit formula:

$$\Phi_{CR1} = \frac{I}{2K} R_e^2 f_1(A(\xi), L), \quad (26)$$

where $f_i = f_i(A(\xi), L)$ is a function of foam morphology, which gives its dependence on the skeleton material. For a uniform cross-section the solution can be expressed as a square function of foam relative density ϕ :

$$\Phi_{CR1} = \frac{1}{2K} \sigma_{CR1}^2 = \frac{1}{2K} R_e^2 \left(\frac{4A}{\sqrt{3}L^2} \right)^2 = \frac{2}{K} R_e^2 \cdot \phi^2 \quad (27)$$

The second proper state: We consider uniaxial tension of a specimen for which a stress deviator is given below; energy density as a scalar isotropic function of tensor arguments does not depend on the deviatoric state of stress and orientation of a representative cell:

$$\underline{S} = \begin{bmatrix} \frac{2}{3}\sigma_x & 0 & 0 \\ 0 & -\frac{1}{3}\sigma_x & 0 \\ 0 & 0 & -\frac{1}{3}\sigma_x \end{bmatrix} \quad (28)$$

The stress deviator refers only to shear forces present in the foam skeleton and equaling:

$$F_{\tau}(\underline{S}) = \frac{\sqrt{6}L^2}{4} \sigma \quad (29)$$

in each strut. It also gives a maximum value of normal stress due to the bending moment being the sole non-zero stress component:

$${}^s\sigma_{\xi}(\underline{S}) = \frac{\left(F_{\tau} \frac{L}{2} \right) \left(\frac{2}{3} \left(\frac{t_{max}\sqrt{3}}{2} \right) \right)}{J_{y\max}} = \frac{\sqrt{2}L^3 t_{max}}{8J_{max}} \sigma_x, \quad (30)$$

The symbols t_{max} , J_{max} characterize the strut cross-section in the node and denote respectively a side-length of the triangle or Plateau border and the moment of inertia.

When normal stress reaches the critical value ${}^s\sigma_{\xi CR} = R_e$ the respective critical value of tensile stress can be obtained from the relation:

$$\sigma_{XCR2} = \sigma_{CR}(\underline{S}) = R_e \cdot \frac{8J_{y\max}}{\sqrt{2}L^3 t_{max}} \quad (31)$$

For the second proper state we also obtain a formula that shows the dependence of energy density on the foam material and morphology.

$$\Phi_{CR2} = \frac{1}{4G} (\underline{S}_{CR2} \cdot \underline{S}_{CR2})^2 = \frac{1}{4G} R_e^2 f_2(A(\xi), L) \quad (32)$$

For a uniform cross-section the solution is as follows:

$$\Phi_{CR2} = \frac{1}{4G} (\underline{S}_{CR2} \cdot \underline{S}_{CR2})^2 = \frac{1}{G} R_e^2 \frac{16J^2}{3L^6 t^2} \quad (33)$$

We can calculate the critical values of energy density for considered macroscopic foam when its relative density and elastic moduli as well as geometric parameters and elasticity limit R_e for a solid skeleton are given. Then the energy-based criterion (19) can be verified experimentally.

3 Conclusion

The present paper provides an example of a construction of an effective model of linear elasticity, in which necessary material characteristics such as elastic moduli and elastic limit are calculated basing on an appropriate microstructural model and elementary interactions between the material micro constituents. The derived formulas (25) and (33) for the critical energy density specify its dependence on material and geometric parameters of the solid skeleton morphology. In this way, we obtain a general multiscale algorithm for linear analysis of each type of a foam microstructure modelled with strut systems. This makes it possible to design and manufacture new foam materials according to the assumed requirements. It is also feasible to extend the presented analysis for closed-cell foams; in such a case the cell faces can be modelled with plates. The proposed approach can be applied for further studies on foam material mechanics within the framework of a non-linear analysis accounting for the logarithmic strain measure and plastic hinges.

Acknowledgement

We gratefully acknowledge Miss Anna Strek's diligence and sense of humour while making this text more reader-friendly.

References

- Beltrami, E.: Sulla condizioni di resistenza dei corpi elastici, *Rend. Ist. Lomb., II*, 18-27, (1885) (also in: *Opere matem.*, vol. IV, Milano, (1920), 180-189).
- Bertram, A.; Olschewski, J.: Formulation of anisotropic linear viscoelastic constitutive laws by a projection method. In: Freed, A., Walker, K. (eds.), *High temperature constitutive modelling: theory and application*, ASME, MD-vol. 26, AMD-vol. 121, (1991), 129-137.
- Bikerman, J.J.: *Foams*, Springer-Verlag, New-York, (1973), 33-64.
- Choi, J.B.; Lakes, R.S.: Nonlinear analysis of the Poisson's ratio of negative Poisson's ratio foams, *J. Composite Mater.*, 29, (1995), 113-128.
- Gent, A.N.; Thomas, A.G.: Mechanics of foamed elastic materials, *J. Appl. Polymer Sci.*, 1, (1959), 107-113.
- Gent, A.N.; Thomas, A.G.: Mechanics of foamed elastic materials, *Rubber Chemistry and Tech.*, 36, (1963), 597-610.
- Gibson, L.J.; Ashby, M.F.: The mechanics of three-dimensional cellular materials, *Proc. Roy. Soc. Lond.*, A382, (1982), 43-59.
- Gibson, L.J.; Ashby, M.F.: *Cellular Solids*, 2nd edition, Cambridge University Press, (1998).
- Huber, M.T.: Specific work of strain as a measure of material effort – A contribution to foundations of strength of materials theory, *Czasopismo Techniczne*, XXII, (1904), Nr. 3., 38-40, Nr. 4., 49-50, Nr. 5., 61-63, Nr. 6., 80-81, Lwów (also: *Works*, II, 3-20, PWN, Warszawa, (1956)) – in Polish.
- Ko, W.L.: Deformation of foamed elastomers, *J. Cellular Plastics*, 1, (1965), 45-50.
- Maxwell J.C.: Origins of Clerk Maxwell's electric ideas described in familiar letters to William Thompson, the letter of 18th December 1856, *Proc. Cambridge Phil. Soc.*, 32, (1936), Part V (also ed. by Sir. J. Larmor, Cambridge Univ. Press, (1937), 31-33).
- Mehrabadi, M.M.; Cowin, C.: Eigentensors of linear anisotropic elastic materials, *Q. Jl Mech. Appl. Math.*, 43, (1990), 15-41.
- Menges, G., Kipschild, F.: Estimation of mechanical properties for rigid polyurethane foams, *Polymer Eng. Sci.*, 15, (1975), 623-627.
- Nalepka, K.; Pecherski, R.B.: Physical foundations of energy-based strength criterion for monocrystals, 311-316, *XXX Szkoła Inżynierii Materiałowej*, Kraków-Ustroń, Jaszowiec, 1-4, X 2002, (J. Pacyno ed.), AGH, Kraków, (2002) – (in Polish).
- Nalepka, K.: Private communication, (...).

- Phillips, R.: *Crystals, Defects and Microstructures. Modelling Across Scales*, Cambridge U.K, Cambridge University Press, (2001).
- Roberts, A.P.; Garboczi, E.J.: Elastic properties of model random three-dimensional open-cell solids, *J. Mech. Phys. Solids*, 50 (2002), 33-53.
- Rychlewski, J.: On Hooke's law, *PMM*, 48, (1984a), 420-435, - in Russian (English translation in *Prik. Matem. Mekhan.*, 48, (1984), 303-314.)
- Rychlewski, J.: Elastic energy decomposition and limit criteria, *Uspekhi Mekh.-Advances in Mech.*, 7, (1984b), 51-80 (in Russian).
- Rychlewski, J.: Unconventional approach to linear elasticity, *Arch. Mech.*, 47, (1995), 149-171.
- Wang, Y.; Cuitiño, A.M.: Three-dimensional nonlinear open-cell foams with large deformations, *J. Mech. Phys. Solids*, 48, (2000), 961-988.
- Warren, W.E.; Kraynik, A.M.: Linear elastic behaviour of a low density Kelvin foam with open cells, *J. Appl. Mech.*, 64, (1997), 787-794.
- Warren, W.E.; Kraynik, A.M.: Foam mechanics: the linear elastic response of two-dimensional spatially periodic cellular materials, *Mechanics of Materials*, 6, (1987), 27-37.
- Warren, W.E.; Kraynik, A.M.: The linear elastic properties of open-cell foams, *J. Appl. Mech.*, 55, 1998, 341-346.
- Zhu, H.X.; Knott, J.F.; Mills, N.J.: Analysis of the elastic properties of open-cell foams with tetrakaidecahedral cells, *J. Mech. Phys. Solids*, 45, (1997) 319-343.

Address: Dr. Malgorzata Janus-Michalska, Prof. Ryszard B. Pecherski, Chair of Strength of Materials, Institute of Structural Mechanics, Faculty of Civil Engineering, Cracow University of Technology, Warszawska 24, 31-155 Krakow, Poland; rpecher@ippt.gov.pl.